DOI:10.1190/segam2020-3418232.1

3D seismic modeling of heterogeneous poorly-consolidated sandstones in shale host rocks

Raisya Noor Pertiwi, University of Aberdeen; Isabelle Lecomte, University of Bergen; David Iacopini, Università degli Studi di Napoli Federico II*

Summary

We investigate the correlation between rock properties and seismic expression in sand-injectite complex within shallow depositional systems. We first upscale 1D microstructural observations to a 3D geological-scale model, and then perform 3D seismic forward modeling. Using an existing theoretical rock-physics investigation in brine- and gas-saturated poorly-consolidated sands as well as illite-dominated shales, we consider the influence of frequency-related behavior as a fundamental part in the upscaling process of sand and shale elastic properties. The 3D synthetic modeling assumes that sands microstructural features are isotropic while shales are vertical transverse isotropic, and is heterogeneous at the field-scale, i.e., shales are finely layered while sands have complex geometry. The seismic modeling results show that the sand intrusions are difficult to detect in the seismic sections because of the small acoustic impedance contrast with the surrounding shales but also due to the irregular features of top and bottom sands, and the complex connectivity between the parent sands with the sand intrusions. Their visibility is further compromised with the effect of complex wave propagation and the interferences of backscatter seismic energy (constructive and destructive) as a result of 3D heterogeneities in shale and sand petrophysical and elastic properties. Therefore, even in the most optimal survey illumination, a careful interpretation of the reflectivity response is still required to predict most sand boundaries.

Introduction

When large volumes of sand injectites are encased in shale host rocks, the sand features are often difficult to detect in the seismic sections. This is due to the small acoustic impedance contrast with the surrounding shales, the irregular features of top and bottom sands, and the complex connectivity between the parent sands and the sand intrusions. As a first attempt to understand the seismic response of a sand injectites complex, we create 3D synthetic facies and petrophysical models for two different scenarios, i.e., where sands are fully-saturated with brine or gas. For each case, the sands are considered isotropic while shales have vertical transverse isotropy (VTI) microstructural features. The model corresponds to a shallow-depth environment case, where poorly-consolidated sand intrusions with complex geometries are encased in finely layered illite-dominated shale host rocks. Seismic modeling is then performed to understand the implications of bulk density and acoustic velocity variations in each lithology, which in turn are a product of variations in textural factors, e.g., mineralogy, grain shapes and orientations; and non-textural parameters, e.g., fluid content and burial depth. This study considers the frequency-related elastic behavior as a fundamental part in the upscaling process from microstructural observations to a 3D geological-scale model.

Methodology

Our workflow consists of 3D petrophysical and elastic modeling of sands and shales, followed by 3D forward seismic modeling. We use the sand elastic model of Pertiwi et al. (2020) to model the poorly-consolidated sand elastic properties. The empirical model of Pertiwi et al. (2020) represents the dry elastic modulus of quartz dominated sands as a function of porosity, fluid saturation, and pressure at low- and high-frequency regimes, e.g., 1 Hz and 500 kHz, respectively, which enables the low-frequency elastic model of poorly-consolidated sandstones to be elucidated for various pressure regimes. The dry sand elastic model at a consolidation pressure of 15 MPa is selected for this study, where it reflects 1-2 km burial depth, consistent to the depth of interest in our 3D model. The saturated-sand elastic model is then calculated for two pore-fluid types, i.e., brine and gas, using Gassmann's formula. Furthermore, the elastic stiffness of shales in low- frequency regime is calculated by using the inclusion-based modeling as shown in Pertiwi et al. (2020), which assumes the inclusion of silt to cause disruption on the alignment of clay particles. Along with porosity, clay volume, and density, the rearrangement of the clay structural orientation (quantified as orientation distribution function – ODF), is an important variable for the computation of elastic models.

Following the 1D low-frequency model, we transform the observation model into a 3D field-scale model. In the 3D model, six synthetic log datasets are created to contain lithology information, porosity, density, and clay-content. Here, the porosity for each lithology is also designed to be coherent with a porosity-depth trend, where the increasing burial depth reduces the porosity of shales and sands. By using the log datasets, we later perform petrophysical and facies modeling in order to model the spatial distribution of petrophysical parameters and sand geometries, where we consider the sands to have an isotropic behavior and shales an intrinsic VTI behavior. The resulting 3D shale and sand elastic models are designed to replicate the complex clastic reservoir of Barents Sea sedimentary basins, where the sands are poorly-consolidated and under normal compaction (e.g., Yenwongfai et al., 2017). In the field-scale, the 3D synthetic model is heterogeneous due to the geometrically complex sand intrusions encased in thinly-layered shales. The sand

DOI:10.1190/segam2020-3418232.1

intrusions geometry is designed with complex variations of thickness, orientation, and sizes of sand intrusions, as well as variations in size of parent sand bodies and distance between intrusions. The sand bodies may consist of a single unit or several units of parent sands with interconnecting sills like sands, as reflected in the geometry of sandstone intrusion complex, e.g., in Volund field (cf. Braccini et al., 2008). In this modeling experiment, the modeled sand bodies vary in thickness between 10 to 200 m and dip between 0^0 to 40^0.

Following the facies and petrophysical modeling, we perform seismic modeling to analyze the reflectivity/seismic responses in a heterogeneous isotropic medium. Here, the available information of shales intrinsic anisotropy is not accounted in the seismic modeling. The seismic modeling is performed by the 3D Point-Spread Function (PSF) based convolution introduced by Lecomte et al. (2003) to simulate prestack-depth migrated (PSDM) seismic. In the simulation, we assume a perfect illumination (all reflector dips being illuminated) to first analyze the overall detectability of the structures, and a 40-Hz dominant frequency that coherent to resolution threshold ($\lambda/4$) of 12.5 m. The method can be adapted to a lower lateral resolution as often encountered in real cases, e.g., $\lambda/2$.

Results and Discussions

The 3D synthetic model corresponds to shallow depth intervals of 1-2 km, i.e., equivalent to 10-20 MPa compaction. Each petrophysical and elastic parameter of the synthetic model matches the trend and range of experimental and well-log datasets that describe poorly-consolidated sands and illite-rich shales properties (Figure 1 and 2). For example, the results of poorly-consolidated sands modeling agree with the porosity, density, and elastic properties trend investigated by Blangy et al. (1993), while the elastic response of the modeled shales follows various observations in illite-dominated shales with approximately >30% clay mineral at given depth range (e.g., Nooraiepour et al., 2017).

The elastic properties of poorly-consolidated sands are strongly determined by porosity and pore-fluid types (Figure 1). For example, in a vertical P-wave velocity (Vp) versus vertical S-wave velocity (Vs) crossplot, the gas-saturated sand trend deviates away from the shale trend, while the brine-saturated sands show a similar trend with shales. Meanwhile, for shales, the relationship between clay-percentage and porosity is an important constraint to determine its elastic parameters. Therefore, during the petrophysical modeling, the porosity model of shales requires additional parameters such as silt and clay volumes in addition to the porosity-depth trend. Here, a prediction bound is proposed to provide the correlation between clay volume and porosity, with an assumption that the configuration of clay particles will determine the framework and hence the porosity of the mixtures (Figure 2a). The clay concentration in shales is also important to determine the preferred orientation of clay or ODF, assuming that the variation of burial effective stress or compaction is small (Figure 2b). The decreasing values of ODF demonstrate the disruption of pure-clay composites due to the increase of silt content. As a result, the porosity, clay volume, and ODF are important variables to determine the elastic parameters of shales. Figure 3a and 3b show the example of the clay concentration and porosity modeling results, where these values along with the pore-fluid properties within sands will determine the P-impedance values (Figure 3c and 3d).

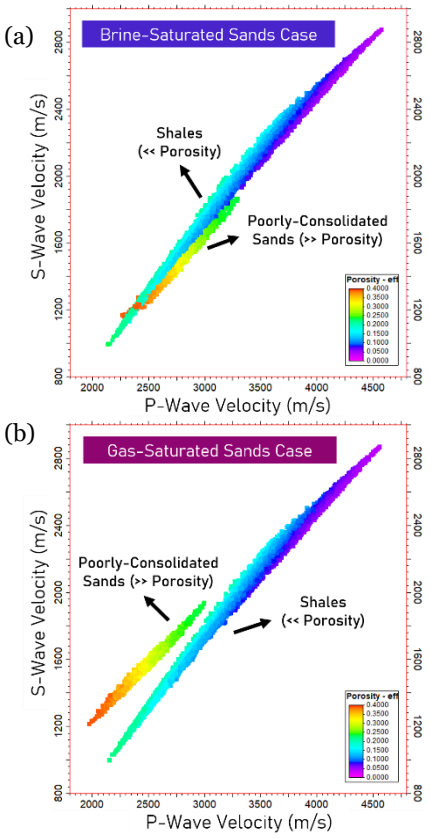

Figure 1 The crossplot from 3D model points between Vp and Vs as a function of porosity for scenario of (a) brine-saturated sands encased in shales, and (b) gas-saturated sands encased in shales.

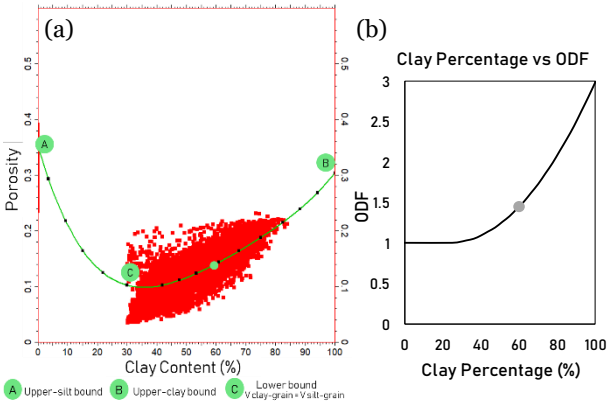

Figure 2 (a) The crossplot from 3D model points between clay-content and porosity in shales, and (b) the relationship between orientation distribution function (ODF) with the clay-content.

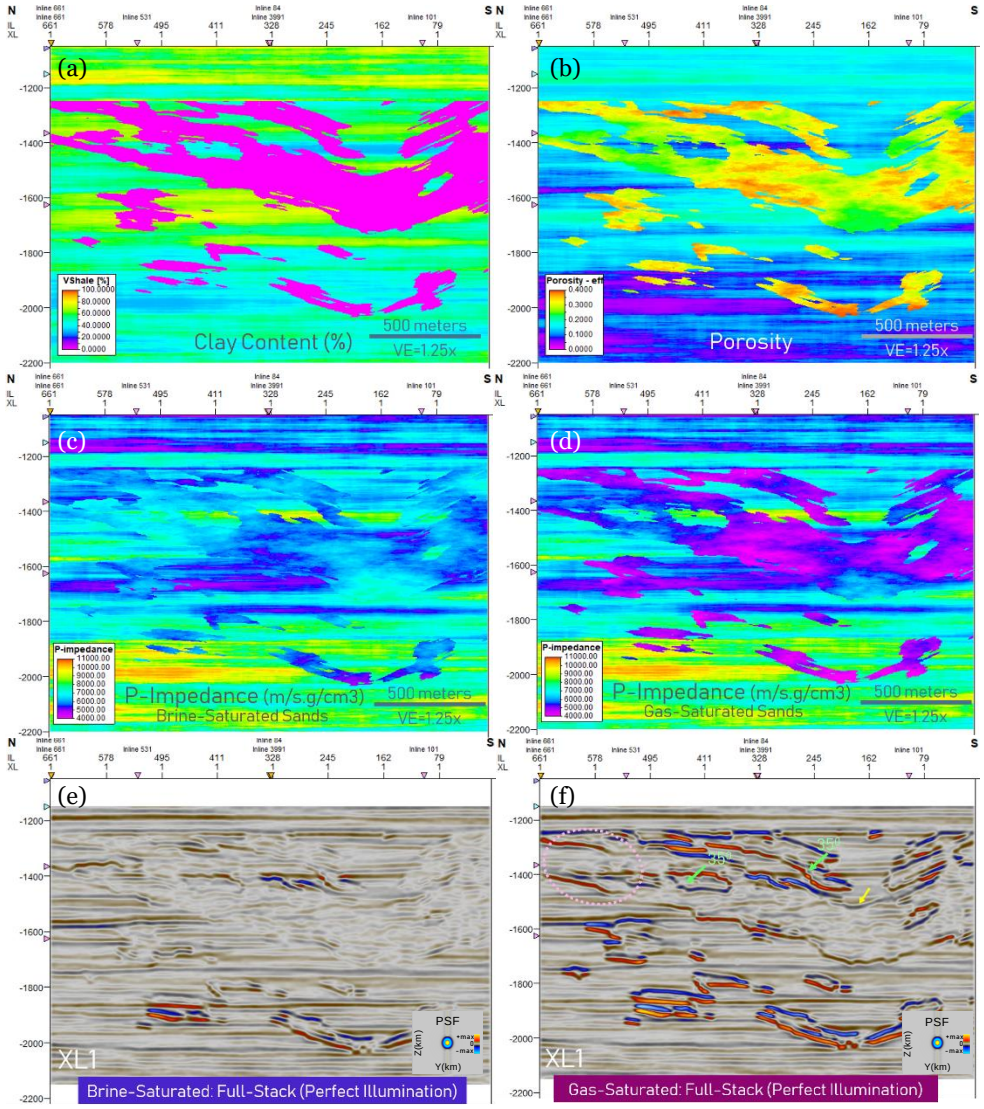

Figure 3 A cross-section showing the (a) clay content, (b) porosity, (c) P-impedance response on brine- and (d) gas-saturated sands scenario, and (e) full-stack PSDM seismic on brine- and (f) gas-saturated sands scenario.

The seismic modeling results indicate that the detectability of a sand interface relates to a more complex interference pattern than just related to the sand-body thickness, as the complex wave propagation and interference of backscatter seismic energy caused by elastic and petrophysical variation, hence the impedance contrasts with the overlying/underlying strata are also strongly controlling the seismic responses. For example, the amplitude across the top- and base gas-saturated sands will most likely have negative and positive amplitude, respectively, yet amplitude variations (e.g., zero amplitudes) may be expected due to the petrophysical heterogeneities found in the sand intervals and the host rocks (Figure 3f and 4c, yellow arrows). In addition, the elastic properties of poorly-consolidated sands are strongly determined by the pore-fluid types. When the sand bodies are saturated with brine, the acoustic-impedance contrasts with its surrounding shale host rocks are low and consequently difficult to identify in seismic responses (Figure 3e, 4b, and 5b). Meanwhile, the higher impedance contrasts between gas-saturated sands and the shales background cause stronger reflections on the sand-shale boundaries (Figure 3f, 4c, and 5c). Although the impedance contrast is relatively strong for gas-saturated sands, the effect of heterogeneity in the impedances often causes their seismic responses to appear subtle even with the most optimal subsurface illumination used here (Figure 3f, pink circle). Moreover, when the vertical spacing between the intrusions is small, e.g., closely-stacked sills, they often appear in seismic as connected bodies (Figure 4c, pink circle). In XY sections, the effect of spatial variability of impedances also cause the gas-saturated sand boundaries to generally exhibit subtle seismic responses, similar to the common responses found in the

brine-saturated sand boundaries (Figure 5b and 5c, white arrows). Several dipping intrusions may be challenging to detect, especially in brine-saturated sand case where their seismic responses are resembling fault features rather than discordant layers (Figure 4b, white arrows). This, and previous evidences further suggest that the complex architectures of sand injectites may raise the potential of misinterpreting seismic responses. However, in this modeling example, a large number of thin sand bodies with relatively steep dip angle can still be properly imaged in the gas-saturated sand case (Figure 3f and 4c, green arrows). Additional modeling with limitations in illumination should be carried out as a comparison to the results presented here.

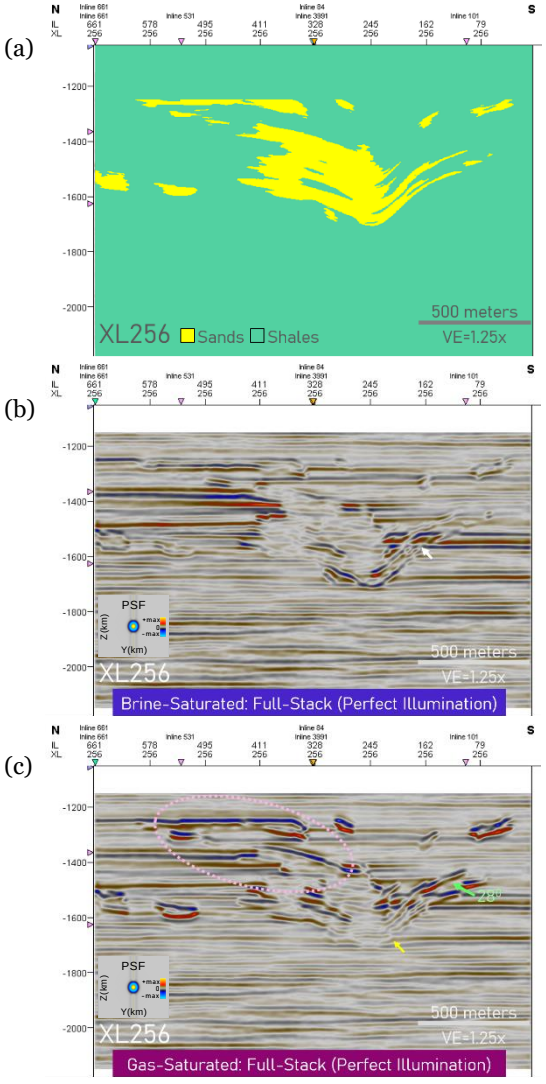

Figure 4 (a) Lithological distribution, and full-stack PSDM seismic for (b) brine- and (c) gas-saturated sands scenario in XL 256.

Conclusions

A 3D synthetic model, containing petrophysical, elastic, and seismic model, is designed to represent a case of poorly-consolidated sand intrusions encased in illite-dominated shale host rocks at shallow depths. A multifrequency rock-physics model is implemented during the upscaling of microstructural observations, i.e., shale and sand elastic properties, to a field-size model. The synthetic model provides realistic petrophysical properties, e.g., porosity and clay-volumes, and elastic properties in a complex geometry environment of sand intrusions. The resulting 3D PSDM seismic volumes highlight significant implications of the petrophysical heterogeneities, variation in pore-fluid types, and complex architectures of sand injectites in interpreting the seismic amplitude responses.

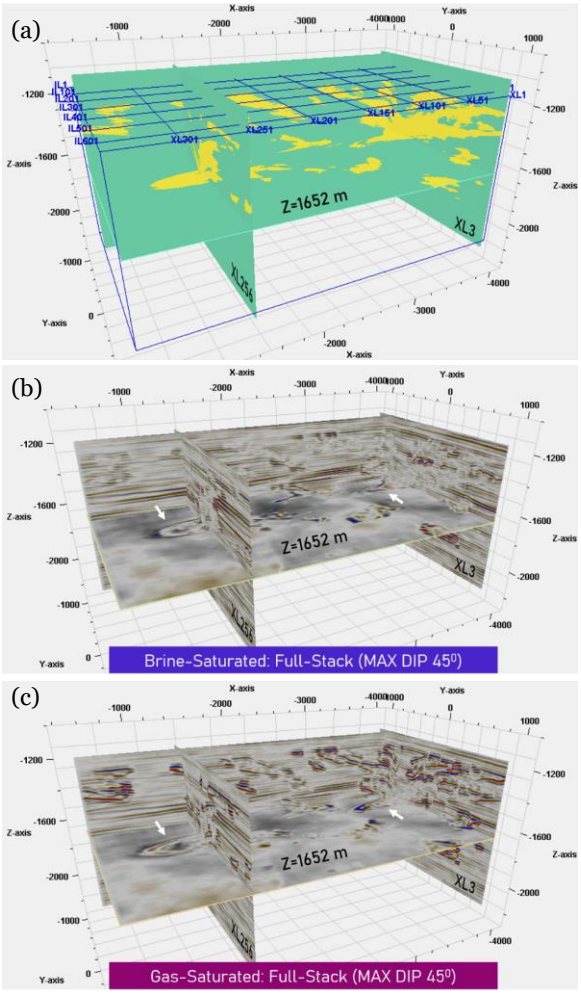

Figure 5 (a) Lithological distribution, and full-stack PSDM seismic for (b) brine- and (c) gas-saturated sands scenario in a 3D volume.

Acknowledgments

The authors thank LPDP Indonesia (S-1334/LPDP.3/2018), NORSAR Innovation, and Sand Injection Research Group for their support.

REFERENCES

Blangy, J., S. Strandenes, D. Moos, and A. Nur, 1993, Ultrasonic velocities in sands — Revisited: Geophysics, **58**, no. 3, 344–356, doi: https://doi.org/10.1190/1.1443418.

Braccini, E., W. De Boer, A. Hurst, M. Huuse, M. Vigorito, and G. Templeton, 2006, Sand injectites: Oilfeld Review, **20**, 34–49.

Lecomte, I., H. Gjøystdal, and Å. Drottning, 2003, Simulated prestack local imaging — A robust and efficient interpretation tool to control illumination, resolution, and time-lapse properties of reservoirs: SEG 73rd Annual Meeting, Expanded Abstracts, 1525–1528, doi: https://doi.org/10.1190/1.1817585.

Nooraiepour, M., N. H. Mondol, H. Hellevang, and K. Bjørlykke, 2017, Experimental mechanical compaction of reconstituted shale and mudstone aggregates — Investigation of petrophysical and acoustic properties of SW Barents Sea cap rock sequences: Marine and Petroleum Geology, **80**, 265–292, doi: https://doi.org/10.1016/j.marpetgeo.2016.12.003.

Pertiwi, R.N., D. Iacopini, and D. Healy, 2020, Effective medium model in shales and sandstones at multifrequency observations, extended abstract: Fifth EAGE Workshop on Rock Physics, Extended Abstracts, RP17.

Yenwongfai, H. D., N. H. Mondol, J. I. Faleide, and I. Lecomte, 2017, Prestack simultaneous inversion to predict lithology and pore fluid in the Realgrunnen Subgroup of the Goliat Field, southwestern Barents Sea: Interpretation, **5**, SE75–SE96, doi: https://doi.org/10.1190/INT-2016-0109.1.